Letter

Magnetic field induced Anderson localization in the orbital-selective antiferromagnet $BaMn_2Bi_2$

Takuma Ogasawara,[1] Kim-Khuong Huynh,[2,*] Stephane Yu Matsushita,[2] Motoi Kimata,[3] Time Tahara,[4] Takanori Kida,[4] Masayuki Hagiwara,[4] Denis Arčon,[5,6] and Katsumi Tanigaki[2,7,†]

[1]*Department of Physics, Graduate School of Science, Tohoku University, 6-3 Aoba, Aramaki, Aoba-ku, Sendai 980-8578, Miyagi, Japan*
[2]*Advanced Institute for Materials Research (WPI-AIMR), Tohoku University, 1-1-2 Katahira, Aoba, Sendai, 980-8577 Miyagi, Japan*
[3]*Institute for Materials Research, 1-1-2 Katahira, Aoba, Sendai, 980-8577 Miyagi, Japan*
[4]*Center for Advanced High Magnetic Field Science, Graduate School Science, Osaka University, 11 Machikaneyama, Toyonaka, 560-0043 Osaka, Japan*
[5]*Faculty of Mathematics and Physics, University of Ljubljana, Jadranska cesta 19, 1000 Ljubljana, Slovenia*
[6]*Jozef Stefan Institute, Jamova cesta 39, 1000 Ljubljana, Slovenia*
[7]*BAQIS, Building 3, No. 10 Xibeiwang East Road, Haidian District, Beijing 100193, China*

(Received 4 January 2022; revised 11 July 2022; accepted 12 July 2022; published 25 July 2022)

We report a metal-insulator transition (MIT) in the half-filled multiorbital antiferromagnet (AFM) $BaMn_2Bi_2$ that is tunable by a magnetic field perpendicular to the AFM sublattices. Instead of an Anderson-Mott mechanism usually expected in strongly correlated systems, we find by scaling analyses that the MIT is driven by an Anderson localization. Electrical and thermoelectrical transport measurements in combination with electronic band calculations reveal a strong orbital-dependent correlation effect, where both weakly and strongly correlated $3d$-derived bands coexist with decoupled charge excitations. Weakly correlated holelike carriers in the d_{xy}-derived band dominate the transport properties and exhibit the Anderson localization, whereas other $3d$ bands show clear Mott-like behaviors with their spins ordered into AFM sublattices. The tuning role played by the perpendicular magnetic field supports a strong spin-spin coupling between itinerant holelike carriers and the AFM fluctuations, which is in sharp contrast to their weak charge coupling.

DOI: 10.1103/PhysRevB.106.L041114

Introduction. A metal-insulator transition (MIT) can occur in a clean solid as a consequence of strong electron-electron correlations that open a Mott pseudogap in the excitation spectrum [1]. On the other hand, quantum interferences arising from disorder in a noninteracting system can destroy all extended states and induce an Anderson localization (AL) transition [2]. The intertwining of these two mechanisms within the same system generates rich phase diagrams containing coexisting complex phases and intriguing critical behaviors at the phase boundaries [3,4]. Theoretical calculations of correlated single-band models at half filling have found that correlated metallic phases can be enhanced in the regime of weak disorder and correlation [3,4]. Intricate Anderson-Mott insulating phases with suppressed Mott-like antiferromagnetic order (AFM) [5] and/or the coexistence of spatially segregated Mott and Anderson regions have been proposed in the regime of strong disorder and correlation [6].

The participation of multiple orbitals often found in transition metal compounds can make the above competitions even more interesting. Orbital-selective Mottness scenarios have been recently put forward to discuss the cases of coexisting weakly and strongly correlated energetic bands, both of which are derived from the same partially filled d shell [7,8]. Unfortunately, Anderson-Mott and AL transitions in the presence of orbitally selective Mottness have been experimentally and theoretically unexplored due to the lack of suitable model systems.

In the present Letter, we combine experimental observations and band calculations to show that with the help of orbital degrees of freedom, the dominant role in such intriguing cases can be taken by an AL mechanism even in the presence of strong electronic correlations. Our model compound is single-crystalline $BaMn_2Bi_2$ [Fig. 1(a)], the end member in the family of half-filled G-type AFM $BaMn_2Pn_2$'s (Pn stands for As, Sb, and Bi) [9–16]. In these materials, structurally similar to their sister $BaFe_2As_2$ with a $3d^6$ electronic shell [7], five $3d$ orbitals are essential to the electronic properties. The correlation strength varies greatly depending on the Mn's $3d$ orbitals, even though $BaMn_2Pn_2$ is at half filling [17,18].

$BaMn_2Bi_2$ exhibits a clear orbital dependence, as its d_{xy}-derived band is virtually unaffected by electronic correlation whereas the other orbitals show very strong Mott-insulating behavior with AFM order [Figs. 1(b) and 1(c)]. The holelike charges in the d_{xy}-derived band exhibit a bad metallic state at high temperatures, but with cooling down undergo a localization transition that renders a weak insulator. Intriguingly, MIT is tunable by a magnetic field that is *perpendicular* to the G-AFM axis ($\mathbf{H}_{ab}$) so that the material becomes metallic at high magnetic field strength H_{ab}. By employing scaling analyses for the conductivities at different H_{ab}, we found that the critical exponent of MIT is $\nu \approx 1.4$. This value corresponds

*huynh.kim.khuong.b4@tohoku.ac.jp
†katsumi.tanigaki.c3@tohoku.ac.jp

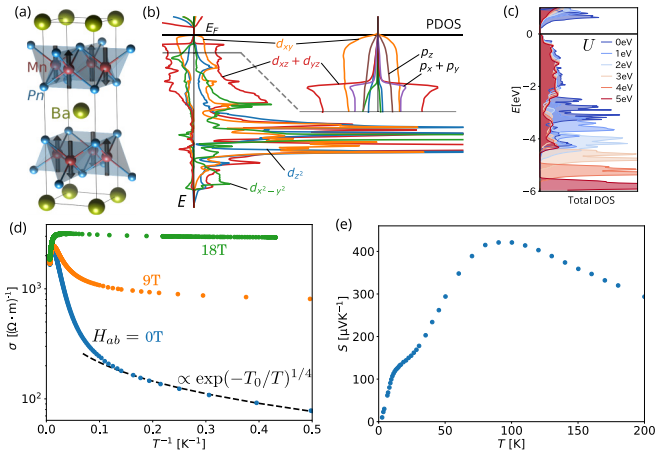

FIG. 1. (a) The crystallographic and magnetic structure of $BaMn_2Pn_2$. (b) Spin-polarized PDOS of Mn's $3d$ and Bi's $6p$ orbitals calculated for $U = 0$ at a Mn site in the spin-up AFM sublattice. The inset on the right-hand side enlarges the region near the E_F. (c) U heavily affects all bands except the d_{xy}-derived one close to the E_F. (d) The electrical conductivity of $BaMn_2Bi_2$ measured in a perpendicular magnetic field $\mathbf{H}_{ab} \perp \hat{c}$ configuration. The black dashed line is the fit to the VRH model. (e) The temperature dependence of the Seebeck coefficient of $BaMn_2Bi_2$ at zero magnetic field.

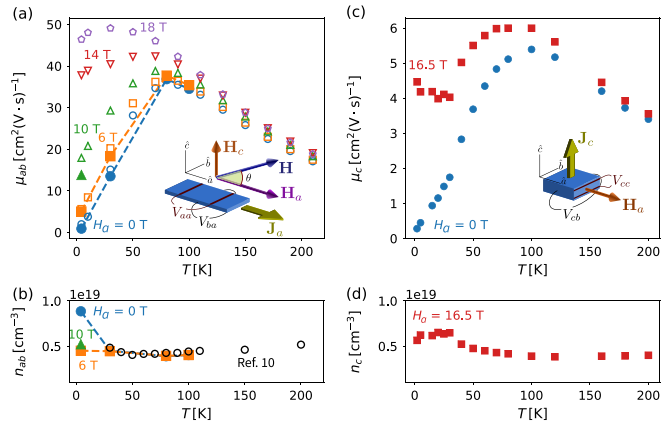

FIG. 2. (a) Effects of H_a on temperature dependencies of carrier mobility in the *ab* plane (μ_{ab}) estimated from the crossed-field Hall measurements [20]. (b) Carrier number estimated from the high-H_c Hall coefficient. The black open circles represent the carrier estimated from the single field transverse Hall measurement published in Ref. [15]. (c) Temperature dependencies of carrier mobility along the $\hat{c}$ axis (μ_c) estimated for $H_a = 0$ and 16.5 T. (d) Carrier number estimated from the high-H_a Hall coefficient. More details for the Hall measurements can be found in the Supplemental Material (SM) [20].

to an AL transition, but not a Anderson-Mott transition, in the unitary universal class and therefore reaffirms the absence of a correlation effect in the d_{xy}-derived band. On the other hand, the unusual tuning role played by $\mathbf{H}_{ab}$ supports a picture of strong coupling between the spin angular momenta of d_{xy} holes and the AFM fluctuations. The contrast in coupling strengths, weak for charge and strong for spin excitations, is reminiscent of the scenario of spin-charge separation recently proposed for multiobital Hund's metal [7,19].

Multiorbital electronic structure and magnetism. Figure 1(b) shows the band structure of $BaMn_2Bi_2$ as obtained from our spin-polarized band calculations [20] by using the program code WIEN2K and QUANTUM ESPRESSO [21,22]. Both "core" and itinerant electronic states coexist. The "core" states locate far away from E_F, and their spins are well ordered into G-AFM sublattices. These AFM-polarized bands show clear Mott-like behaviors because they are effectively pushed down by increasing the correlation strength U [Fig. 1(c)].

Much more important for transport properties is the band at the vicinity of E_F. The partial density of states (PDOS) [Fig. 1(b)] shows that the contribution from the $3d_{xy}$ orbital dominates this band, being 60 and 10 times larger than those from the Mn's $d_{xz/yz}$ and Bi's p_z orbitals, respectively. This d_{xy}-derived band resembles that of a paramagnetic metal. Its wide bandwidth that favors itinerant holes and the PDOS of "spin-up" and "spin-down" states are almost equivalent. Interestingly, we found that the d_{xy}-derived band remains virtually unaffected even for extremely large U [Fig. 1(c)]. Our band calculations show a strong orbital-selective correlation effect in $BaMn_2Bi_2$ and are in a good agreement with the previous calculations and experimental observations for the sister compound $BaMn_2As_2$ [17,18,23]. Whereas other $BaMn_2Pn_2$'s remain insulating under high magnetic fields, $BaMn_2Bi_2$ is in the vicinity of an intriguing field-tuned MIT. The d_{xy}-derived band at the vicinity of the E_F is the playground for interesting transport and magnetism, as described below.

Localization in transport properties and delocalization via $\mathbf{H}_{ab}$. At high temperatures (T) and zero magnetic field, $BaMn_2Bi_2$ exhibits a bad metal behavior which then changes to insulating at $T_{min} \approx 83$ K. Figure 1(d) shows that the conductivity σ follows an insulating Arrhenius law at $T < T_{min}$ and then a three-dimensional variable range hopping (VRH) $\sigma \propto \exp[-(T_0/T)^{1/4}]$ at lower temperatures [15]. The insulating state at low T's has been interpreted as the property of a small semiconductinglike band gap [10,13]. However, the Seebeck coefficient (S) of $BaMn_2Bi_2$ approaches zero as $T \to 0$ [Fig. 1(e)]. The contrast behaviors of $\sigma(T)$ and $S(T)$ demonstrate an AL of finite DOS at E_F [24].

The insulating behavior of $BaMn_2Bi_2$ is effectively suppressed by $\mathbf{H}_{ab}$ [Fig. 1(d)]. The delocalization effect is isotropic with respect to the direction of $\mathbf{H}_{ab}$ in the crystallographic *ab* plane [14,15]. Meanwhile, magnetic fields parallel to the AFM axis ($\mathbf{H}_c$) result in a much smaller effect [14–16]. The in-plane magnetic field $\mathbf{H}_{ab}$ is thus the tuning parameter for the AL transition in $BaMn_2Bi_2$.

Hall effects. In an AL state and/or in the vicinity of an AL transition, the Hall effect is a complex quantity that remains not well understood [24–29]. In $BaMn_2Bi_2$, the ability to accurately control the AL transition in the same sample via the $\mathbf{H}_{ab}$ provides a good opportunity to study the interesting topic. We employed a crossed-field measurement method to investigate the current-in-plane Hall effect [20,30]. As schematically shown by the inset of Fig. 2(a), $\mathbf{H}_c$ is the probing field that helps to measure the transverse Hall response from the electronic state that is *tuned by* $\mathbf{H}_a$. The effect of $\mathbf{H}_a$ on the Hall resistivity $\rho_{ba}(H_c)$ was investigated by rotating the sample in different static $\mathbf{H}_a$'s [20]. The crossed-field measurements revealed tuning effects for $\mathbf{H}_a$ on ρ_{ba} [20]. At low H_a, the $\rho_{ba}(H_c)$ curves show a nonlinearity that is related to the VRH

transport regime [24]. In the metallic state at high H_a and/or high T, the nonlinearity disappears and ρ_{ba} returns to a simple linear line.

The crossed-field Hall measurements also allowed us to estimate the effects of $\mathbf{H}_a$ on the carrier number and mobility. Figure 2(a) shows that the in-plane mobility μ_{ab} displays a broad peak corresponding to the MIT at $T_{\min}$ and then decreases to zero when entering the VRH regime. At high H_{ab}, μ_{ab} is metallic down to low T. The carrier number n_{ab} is not affected by both H_a and T [Fig. 2(b)].

Similar effects of H_a can be obtained from the out-of-plane Hall effect [inset of Fig. 2(c)], in which $\mathbf{H}_a$ takes a dual role of being the Hall and the tuning fields [20]. As shown in Fig. 2(c), $\mathbf{H}_a$ effectively removes the insulating behavior at zero magnetic field of the interlayer mobility μ_c. On the other hand, the interlayer carrier number n_c, estimated at $H_a \geqslant 15$ T, does not change with T [Fig. 2(d)]. These deduced μ_{ab} and μ_c corroborate a clear delocalizing effect of $\mathbf{H}_{ab}$ on the d_{xy} holes.

Scaling analyses. Since the localization transition in the d_{xy}-derived band is tunable via $\mathbf{H}_{ab}$, one may anticipate that at $T = 0$ there exists a quantum critical point $H_{\rm cr}$ separating the metallic and insulating phases. Using the scaling theory for the localization in both metallic and insulating regions [31,32], we investigated the criticality of the in-plane conductivity in the window $0.5\,\mathrm{K} \leqslant T \leqslant 1\,\mathrm{K}$ by tuning H_a [33].

At finite temperatures, the in-plane conductivity measured under various H_a's should obey the rule $\sigma(h,T) = T^{\alpha}\mathcal{F}(h/T^{\beta})$. Here, $h = H_a/H_{\rm cr} - 1$ is the dimensionless distance of magnetic field from the critical field $H_{\rm cr}$, and h/T^{β} is the only variable of the scaling function $\mathcal{F}$. At the vicinity of $H_{\rm cr}$, the localization (correlation) length ξ diverges as $|H_a - H_{\rm cr}|^{-\nu}$. The critical exponents α and β are related to the correlation length exponent ν_1 and the dynamical exponent z by $\alpha = (d-2)z^{-1} = z^{-1}$ and $\beta = (z\nu_1)^{-1}$, in which the $d = 3$ is the dimensionality of the system. Figure 3(a) shows that the best scaling is achieved with $\alpha \approx 0.503$ and $\beta \approx 0.355$, corresponding to $z = \alpha^{-1} \approx 1.988$ and $\nu_1 = \alpha\beta^{-1} \approx 1.415$, by a polynomial fitting near $h = 0$ [34]. The fitting also yields the critical field $H_a^{\rm cr} \approx 5.07$ T [20].

On the other hand, at $T = 0$, the two sides across $h = 0$ exhibit entirely different states. For the metallic state at $h > 0$, the zero-temperature conductivity σ_0 is positive and finite, however, $\sigma_0 < 0$ in the insulating region, $h < 0$. We thus employed a different approach for each region. For $h > 0$, the metallic conductivity generally obeys $\sigma_0(h) \propto h^{\mu}$. The critical exponent is related to ν by the definition $\mu = (d-2)\nu_2 = \nu_2$. We estimated σ_0 from the power-law fitting $\sigma(T,H_a) = \sigma_0(H_a) + aT^q$ at low temperatures; q takes a value close to the inverse of the dynamical exponent in the finite-temperature scaling, i.e., $q \approx 1/z \approx 0.5$ [31,32]. The fitting of obtained σ_0's to the critical law $\sigma_0 \propto h^{\nu_2}$ [black line in the metallic region of Fig. 3(b)] yields $\nu_2 \approx 1.39$.

As shown in Fig. 3(b), in the insulating side ($h < 0$) at $T = 0$ K, the scaling behavior appears in the H_a dependence of T_0 extracted from the modified VHR law $\sigma(T) \propto T^{1/2}\exp[-(T_0/T)^{1/4}]$ [34]. As a result of the small T_0 near $h = 0$, the T dependence of the prefactor is taken into account [20]. By definition, $T_0 \propto \xi^{-3}$, and ξ diverges as $|h|^{-\nu_3}$

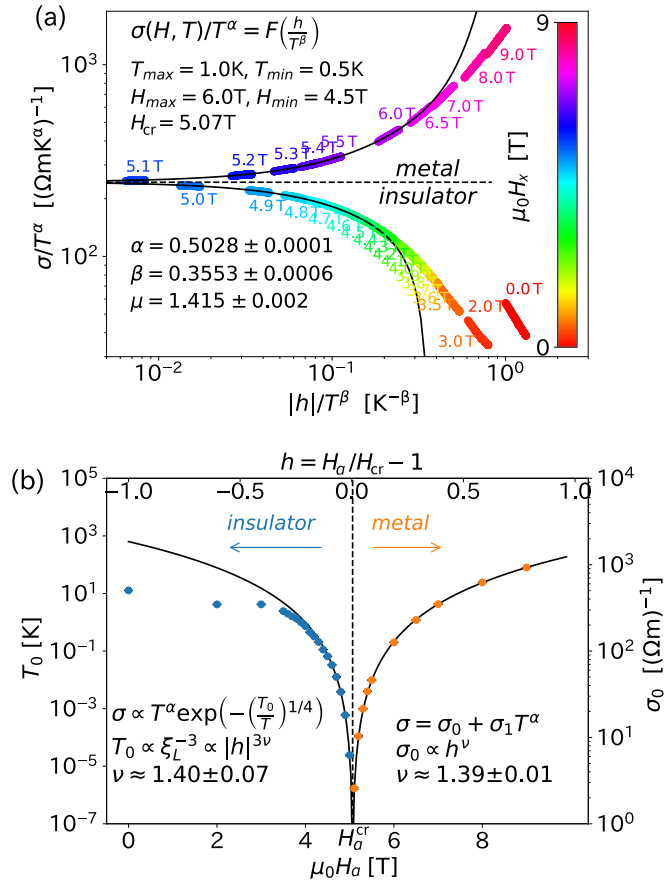

FIG. 3. Scaling properties of the MIT. (a) Finite-temperature scaling properties of $\sigma(T,H_a)$. The solid circles the represent the $\sigma(T)$ data measured at H_a's as shown in the text and the color bar. The solid lines are the fit using a polynomial expansion of $\mathcal{F}$ [20,33]. (b) Scaling properties of σ_0 in the metallic region and T_0 in the VRH insulating regime. The solid lines are power-law fittings [20,33]. $T_{\max}$ ($H_{\max}$) and $T_{\min}$ ($H_{\min}$) in (a) indicate the fitting range in T (H_a). The scaling formulas for each scaling are also shown.

as $h \to 0$. A $T_0 \propto |h|^{3\nu_3}$ fit (black line) yields $\nu_3 = 1.40$. The deviations from the fittings at $H_a < 3$ T in Figs. 3(a) and 3(b) are mainly due to the effect of an additional positive magnetoresistance [14,15] that is not included in the scaling theory.

The obtained values $\nu_i \approx 1.4$ point to an AL transition that belongs to the 3D unitary universality class, for which a $\nu^{\rm cal} \approx 1.4$ was obtained by simulations [35–37]. This is consistent with the absence of time-reversal symmetry caused by both the tuning parameter h and the G-AFM order. The value $\nu \approx 1.4$ is also far from the critical exponent of an Anderson-Mott transition $\nu = 0.33$ for Cr-doped V_2O_3, and $\nu z = \beta^{-1} = 0.56$ as obtained from theoretical calculations [38,39]. Randomness plays a decisive role and electron-electron interactions are of less importance despite the strong electron correlations of the G-AFM background.

Discussion and summary. The critical exponent $\nu \approx 1.4$ helps us to place the $\mathbf{H}_{ab}$ induced AL transition in the unitary universality class. A unitary, i.e., broken time-reversal symmetry, AL can originate from the randomness in the phase of the electronic hopping amplitude that is introduced by an internal random gauge field, i.e., the magnetic field [35,40].

Thus, a sufficiently strong external magnetic field can induce a delocalization by suppressing the randomness of the internal vector potential. Because the AL transition is tunable solely via the perpendicular $\mathbf{H}_{ab}$ [14,15], the random gauge field causing it has a close connection to the fluctuations of the Mott-like AFM. It has been known that a perpendicular field $\mathbf{H}_{ab}$ can suppress the G-AFM fluctuations effectively whereas a parallel $\mathbf{H}_{c}$ cannot [41].

In Fig. 1(b), the large energy separation between the d_{xy}-derived band and the $3d$ G-AFM states suggests that the hopping of the quasifree holelike charges at E_{F} can cause only infinitesimal perturbations to the latter. On the other hand, from the viewpoint of spin degrees of freedom, the quasistatic AFM spins and the spins of the d_{xy} holes are still coupled via spin-spin interactions [42]. AFM spin fluctuations hence are inherited as phase randomness of the hopping amplitudes, and an AL of charge can be expected as proposed theoretically [42].

The quasi-one-particle characteristics of the $\mathbf{H}_{ab}$-tuned AL amid strong correlation can be viewed as a consequence of the intriguing multiorbital electronic structure. The itinerancy of the d_{xy}-derived band has been shown to be robust even against large U [18], and this supports a picture having different strengths of charge and spin couplings between the itinerant d_{xy} and the deep AFM states. The current picture of the AL that stems from the interactions between d_{xy} and AFM spins also bears some similarities to a recent theoretical model, in which a quasi-many-body localization is shown to arise from the coupling between coexisting fast and slow particles [43].

Acknowledgments. Measurements of transport properties and magnetism were carried out at the Advanced Institute for Materials Research and High Field Laboratory for Superconducting Materials at Tohoku University, and at the Center for Advanced High Magnetic Field Science at Osaka University via the Visiting Researcher's Program of the Institute for Solid State Physics, the University of Tokyo. We thank K. Nomura, K. Ogushi, T. Sato, T. Aoyama, K. Igarashi, H. Watanabe, Y. Yanase, T. Urata, and T. Arima for fruitful discussions. This work was supported by the CREST project "Thermal Management," and by the Grant-in-Aid for Scientific Research on Innovative Areas "J-Physics" (Grant No. 18H04304), and by JSPS KAKENHI (Grants No. 18K13489, No. 18H03883, No. 17H045326, and No. 18H03858). T.O. is thankful for the financial support from the International Joint Graduate Program in Materials Science (GP-MS) of Tohoku University. This research was partly made under the financial support by the bilateral country research program of JSPS between AIMR, Tohoku University and Jozef Stefan Institute, Slovenia. This work was also supported by World Premier International Research Center Initiative (WPI), MEXT, Japan. D.A. acknowledges the financial support of the Slovenian Research Agency through Grants No. BI-JP/17-19-004, No. J1-9145, and No. J1-3007.

[1] N. Mott, *Metal-Insulator Transitions* (CRC Press, Boca Raton, FL, 2004).
[2] P. W. Anderson, Phys. Rev. **109**, 1492 (1958).
[3] V. Dobrosavljevic, N. Trivedi, and J. M. Valles, Jr., *Conductor Insulator Quantum Phase Transitions* (Oxford University Press, Oxford, U.K., 2012).
[4] K. Byczuk, W. Hofstetter, and D. Vollhardt, Int. J. Mod. Phys. B **24**, 1727 (2010).
[5] K. Byczuk, W. Hofstetter, and D. Vollhardt, Phys. Rev. Lett. **102**, 146403 (2009).
[6] M. C. O. Aguiar, V. Dobrosavljević, E. Abrahams, and G. Kotliar, Phys. Rev. Lett. **102**, 156402 (2009).
[7] L. de' Medici, G. Giovannetti, and M. Capone, Phys. Rev. Lett. **112**, 177001 (2014).
[8] L. de' Medici, J. Mravlje, and A. Georges, Phys. Rev. Lett. **107**, 256401 (2011).
[9] Y. Singh, M. A. Green, Q. Huang, A. Kreyssig, R. J. McQueeney, D. C. Johnston, and A. I. Goldman, Phys. Rev. B **80**, 100403(R) (2009).
[10] Y. Singh, A. Ellern, and D. Johnston, Phys. Rev. B **79**, 094519 (2009).
[11] N. S. Sangeetha, V. Smetana, A.-V. Mudring, and D. C. Johnston, Phys. Rev. B **97**, 014402 (2018).
[12] S. Calder, B. Saparov, H. B. Cao, J. L. Niedziela, M. D. Lumsden, A. S. Sefat, and A. D. Christianson, Phys. Rev. B **89**, 064417 (2014).
[13] B. Saparov and A. S. Sefat, J. Solid State Chem. **204**, 32 (2013).
[14] K.-K. Huynh, T. Ogasawara, K. Kitahara, Y. Tanabe, S. Y. Matsushita, T. Tahara, T. Kida, M. Hagiwara, D. Arčon, and K. Tanigaki, Phys. Rev. B **99**, 195111 (2019).
[15] T. Ogasawara, K.-K. Huynh, T. Tahara, T. Kida, M. Hagiwara, D. Arčon, M. Kimata, S. Y. Matsushita, K. Nagata, and K. Tanigaki, Phys. Rev. B **103**, 125108 (2021).
[16] N. Janša, K.-K. Huynh, T. Ogasawara, M. Klanjšek, P. Jeglič, P. Carretta, K. Tanigaki, and D. Arčon, Phys. Rev. B **103**, 064422 (2021).
[17] M. Zingl, E. Assmann, P. Seth, I. Krivenko, and M. Aichhorn, Phys. Rev. B **94**, 045130 (2016).
[18] L. Craco and S. S. Carara, Phys. Rev. B **97**, 205114 (2018).
[19] X. Deng, K. M. Stadler, K. Haule, A. Weichselbaum, J. von Delft, and G. Kotliar, Nat. Commun. **10**, 2721 (2019).
[20] See Supplemental Material at http://link.aps.org/supplemental/10.1103/PhysRevB.106.L041114 for information on the crystal growth, sample preparation, measurement configurations, band calculations, and details of Hall effects and scaling analyses.
[21] P. Blaha, K. Schwarz, F. Tran, R. Laskowski, G. K. H. Madsen, and L. D. Marks, J. Chem. Phys. **152**, 074101 (2020).
[22] P. Giannozzi, S. Baroni, N. Bonini, M. Calandra, R. Car, C. Cavazzoni, D. Ceresoli, G. L. Chiarotti, M. Cococcioni, I. Dabo, A. D. Corso, S. de Gironcoli, S. Fabris, G. Fratesi, R. Gebauer, U. Gerstmann, C. Gougoussis, A. Kokalj, M. Lazzeri, L. Martin-Samos *et al.*, J. Phys.: Condens. Matter **21**, 395502 (2009).
[23] W.-L. Zhang, P. Richard, A. van Roekeghem, S.-M. Nie, N. Xu, P. Zhang, H. Miao, S.-F. Wu, J.-X. Yin, B. B. Fu, L.-Y. Kong,

T. Qian, Z.-J. Wang, Z. Fang, A. S. Sefat, S. Biermann, and H. Ding, Phys. Rev. B **94**, 155155 (2016).
[24] N. F. Mott and E. A. Davis, *Electronic Processes in Non-Crystalline Materials*, 2nd ed., The International Series of Monographs on Physics (Oxford University Press, Oxford, UK, 2012), Sec. 2.13.
[25] L. Friedman, J. Non-Cryst. Solids **6**, 329 (1971).
[26] L. Friedman, Philos. Mag. **36**, 553 (1977).
[27] E. Arnold, Appl. Phys. Lett. **25**, 705 (1974).
[28] L. Fleishman and P. W. Anderson, Phys. Rev. B **21**, 2366 (1980).
[29] N. F. Mott, J. Phys. C **13**, 5433 (1980).
[30] S. Paschen, T. Lühmann, S. Wirth, P. Gegenwart, O. Trovarelli, C. Geibel, F. Steglich, P. Coleman, and Q. Si, Nature (London) **432**, 881 (2004).
[31] F. J. Wegner, Z. Phys. B: Condens. Matter **25**, 327 (1976).
[32] D. Belitz and T. R. Kirkpatrick, Rev. Mod. Phys. **66**, 261 (1994).
[33] P. Virtanen, R. Gommers, T. E. Oliphant, M. Haberland, T. Reddy, D. Cournapeau, E. Burovski, P. Peterson, W. Weckesser, J. Bright, S. J. van der Walt, M. Brett, J. Wilson, K. J. Millman, N. Mayorov, A. R. J. Nelson, E. Jones, R. Kern, E. Larson, C. J. Carey *et al.*, Nat. Methods **17**, 261 (2020).
[34] K. M. Itoh, M. Watanabe, Y. Ootuka, E. E. Haller, and T. Ohtsuki, J. Phys. Soc. Jpn. **73**, 173 (2004).
[35] T. Kawarabayashi, B. Kramer, and T. Ohtsuki, Phys. Rev. B **57**, 11842 (1998).
[36] T. Wang, T. Ohtsuki, and R. Shindou, Phys. Rev. B **104**, 014206 (2021).
[37] M. Watanabe, K. M. Itoh, Y. Ootuka, and E. E. Haller, Phys. Rev. B **60**, 15817 (1999).
[38] P. Limelette, A. Georges, D. Jérome, P. Wzietek, P. Metcalf, and J. M. Honig, Science **302**, 89 (2003).
[39] H. Terletska, J. Vučičević, D. Tanasković, and V. Dobrosavljević, Phys. Rev. Lett. **107**, 026401 (2011).
[40] K. Slevin and T. Ohtsuki, Phys. Rev. Lett. **78**, 4083 (1997).
[41] H. Li, Phys. Rev. B **85**, 134426 (2012).
[42] T. Takaishi, K. Sakakibara, I. Ichinose, and T. Matsui, Phys. Rev. B **98**, 184204 (2018).
[43] N. Y. Yao, C. R. Laumann, J. I. Cirac, M. D. Lukin, and J. E. Moore, Phys. Rev. Lett. **117**, 240601 (2016).